Cell

NOX2 Controls Phagosomal pH to Regulate Antigen Processing during Crosspresentation by Dendritic Cells

Ariel Savina,[1] Carolina Jancic,[1] Stephanie Hugues,[1] Pierre Guermonprez,[1] Pablo Vargas,[3] Ivan Cruz Moura,[1] Ana-Maria Lennon-Duménil,[3] Miguel C. Seabra,[2] Graça Raposo,[4] and Sebastian Amigorena[1,*]
[1] Institut Curie, INSERM U653, Immunité et Cancer, 26 rue d'Ulm, 75248 Paris, Cedex 05, France
[2] Cell and Molecular Biology, Division of Biomedical Sciences, Imperial College London, Exhibition Road, London SW7 2AZ, UK
[3] Institut Curie, INSERM U520, Biologie Cellulaire de l'Immunité Tumoral, 26 rue d'Ulm, 75248 Paris, Cedex 05, France
[4] Institut Curie, CNRS-UMR144, Structures et Compartiments Membranaires, 26 rue d'Ulm, 75248 Paris, Cedex 05, France
*Contact: sebastian.amigorena@curie.fr
DOI 10.1016/j.cell.2006.05.035

SUMMARY

To initiate adaptative cytotoxic immune responses, proteolytic peptides derived from phagocytosed antigens are presented by dendritic cells (DCs) to CD8$^+$ T lymphocytes through a process called antigen "crosspresentation." The partial degradation of antigens mediated by lysosomal proteases in an acidic environment must be tightly controlled to prevent destruction of potential peptides for T cell recognition. We now describe a specialization of the phagocytic pathway of DCs that allows a fine control of antigen processing. The NADPH oxidase NOX2 is recruited to the DC's early phagosomes and mediates the sustained production of low levels of reactive oxygen species, causing active and maintained alkalinization of the phagosomal lumen. DCs lacking NOX2 show enhanced phagosomal acidification and increased antigen degradation, resulting in impaired crosspresentation. Therefore, NOX2 plays a critical role in conferring DCs the ability to function as specialized phagocytes adapted to process antigens rather than kill pathogens.

INTRODUCTION

To initiate most cytotoxic immune responses, dendritic cells (DCs) must present proteolytic peptides derived from pathogens or infected cells to naïve CD8$^+$ T lymphocytes (Banchereau and Steinman, 1998). Phagocytosed antigens are presented to CD8$^+$ T lymphocytes through a process called "crosspresentation" (Guermonprez et al., 2002; Heath et al., 2004). Crosspresentation requires antigen transit through endosomes or phagosomes and eventually partial proteolysis before transport to the cytosol and degradation by the proteasome into 8-9 amino acid peptides. These peptides are then translocated into the lumen of the ER or back into specialized mix ER-phagosome compartments and loaded onto major histocompatibility complex (MHC) class I molecules (Cresswell, 2005).

This initial partial degradation of antigens must be tightly controlled, as it could destroy potential peptides for T cell recognition. In phagocytic cells, protein degradation is mediated by a large family of proteases, often referred to as "lysosomal proteases." Most lysosomal proteases have an optimal proteolytic activity between pH 5.5 and 6.5 (Claus et al., 1998). Phagosomes fuse first with early and late endosomes and then with lysosomes, thus acquiring progressively both the acidification machinery and the lysosomal proteases from the endocytic pathway (Claus et al., 1998; Kjeken et al., 2004).

In macrophages, phagosomes acidify very efficiently, reaching pH 5 in the first 30 min of phagocytosis (Hackam et al., 1998; Yates and Russell, 2005). Acidification results in a strong activation of lysosomal proteases, effective microbe toxicity, and protein degradation into amino acids. Acidification is mainly but not uniquely mediated by the vacuolar ATPase (V-ATPase), which translocates protons from the cytosol into the lumen of endosomes, lysosomes, and phagosomes. Protons, however, can also enter phagosomes passively, through conductive channels (DeCoursey et al., 2001; Nanda et al., 1994) or through other transporters such as voltage-gated proton channels (DeCoursey et al., 2003).

In neutrophils, another large protein complex, the NADPH oxidase NOX2, mediates the transfer of electrons across endocytic (and plasma) membranes and also influences the phagosomal pH. This multicomponent enzyme is unassembled and inactive in resting cells but assembles at the phagosomal or plasma membrane in a stimulus-dependent manner (El-Benna et al., 2005; Segal, 2005). Oxidase subunits include cytosolic proteins such as p47*phox*, p67*phox*, p40*phox*, and rac1 or rac2 (depending

on the phagocyte cell type) and an integral membrane heterodimer, the cytochrom b558 (cyt b558), composed of p22*phox* and gp91*phox*. NOX2 activity generates superoxide anions in the phagocytic lumen, which dismutate to produce hydrogen peroxide and other reactive oxygen species (ROS). Production of ROS in neutrophils therefore consumes important amounts of protons, causing a transient but strong alkalinization (reaching pH 8) of the phagosome lumen during the oxidative burst (Jiang et al., 1997; Segal et al., 1981). Very rapidly, however, ROS production stops, phagosome acidification resumes, and the pH drops within 30 min of phagocytosis (Segal, 2005; Segal et al., 1981).

DCs also express NOX2 but at relatively low levels (around 5% of the levels found in neutrophils) (Elsen et al., 2004). The very low levels of ROS production in DCs suggest that NOX2 may not be involved in microbe killing, particularly since DCs' main function is mostly related to the initiation of adaptative immune responses and not to microbe toxicity. Indeed, DCs have developed specific means of control of endocytic functions that allow efficient antigen presentation. These specializations of the endocytic pathway include the regulated transport of MHC molecules (Mellman and Steinman, 2001; Pierre et al., 1997), the transport of antigen from endosomes and phagosomes into the cytosol (Guermonprez and Amigorena, 2005), and the recruitment of ER proteins to phagosomes (Cresswell, 2005; Guermonprez et al., 2003; Houde et al., 2003). Recent results show that DCs bear low levels of lysosomal proteases (Delamarre et al., 2005; Lennon-Dumenil et al., 2002) and that lysosome acidification in immature DCs is inefficient due to limited recruitment of the cytosolic subunits of the V-ATPase to endosomes and lysosomes, as compared to macrophages or mature DCs (Trombetta et al., 2003). DCs' endocytic pathway can therefore be considered as "specialized" antigen presentation compartments rather than purely degradative organelles. To date, however, none of these specializations of the endocytic compartments in DCs was shown genetically to be indispensable for antigen presentation to T cells.

We now describe a novel specific adaptation of DCs' endocytic pathway to the antigen presentation function. NOX2, a major player of innate immunity in neutrophils, is recruited to immature DC phagosomes, causing active and sustained phagosome alkalinization. In NOX2-defective DCs, phagosomal acidification and antigen degradation were increased, causing a defect in crosspresentation. These results provide the first genetic evidence that a specialization of DCs' endocytic pathway, i.e., active alkalinization of phagosomes by NOX2, is required for efficient antigen crosspresentation to $CD8^+$ T cells.

RESULTS

Active Alkalinization in DC Phagosomes

Efficient antigen processing in phagosomes requires the limited and controlled degradation of protein antigens from phagocytosed cells or cell fragments. Generation of the maximal possible array of peptides for loading on MHC molecules without destroying potentially antigenic peptides implicates a precise control of the activity of lysosomal proteases. One of the most direct ways of controlling the activity of lysosomal proteases is certainly by the pH. In order to measure phagosomal pH in DCs accurately, we set up phagosomal pH measurement by flow cytometry (fluorescence activated cell sorter, or FACS). Latex beads were coated with pH-sensitive (fluorescein isothiocyanate, or FITC) and pH-insensitive (FluoProbe647) fluorescent dyes. After different times of phagocytosis of the beads, the fluorescence intensity was quantified using FACS. The ratio in fluorescence intensity between the two dyes reflected the pH in the phagosomal environment, as shown by imposing fixed pH after permeabilization of the cells (Figure S1A).

As shown in Figure 1A, after a 20 min phagocytosis pulse and 30 min of incubation at 37°C (chase), the fluorescence intensity of FITC was much higher in DCs than in macrophage cell line RAW 264.7, indicating that the pH in DC phagosomes was less acidic than in macrophages. By reporting the mean fluorescence intensity in the two cell populations to a standard curve (see Figure S1 and the Experimental Procedures), the actual pH values in phagosomes were determined. As expected, the pH in bone marrow-derived macrophages (BMMO) and RAW 264.7 (Figure 1B) or J774 cells (not shown) was below 6 after a 20 min pulse and a 10 min chase and acidified further over a 3 hr chase, reaching values around pH 5. In contrast, the pH in DC phagosomes was much higher, reaching 7.5 after 60–120 min (Figure 1B). No significant acidification was observed during the first 3 hr of phagocytosis, although the pH did gradually acidify after longer times of phagocytosis (not shown). A similarly alkaline phagosomal pH (around 7.3) was also found in freshly isolated spleen DCs (Figure 1C). Therefore, the pH in DC phagosomes is alkaline and does not acidify significantly in the first 3 hr of phagocytosis.

The previously described ineffective acidification in DC lysosomes (Trombetta et al., 2003) is probably insufficient to account for these results since the phagosomal pH reached values actually higher than the extracellular medium, suggesting the existence of an active mechanism of alkalinization. We reasoned that if such an alkalinization process existed in DCs, it should become more evident upon blockade of the V-ATPase present in DC phagosomes. This hypothesis was addressed by analyzing DCs' phagosomal pH in the presence of ConcanamycinB (ConB, a specific inhibitor of the V-ATPase) (Benaroch et al., 1995; Yilla et al., 1993). As shown in Figure 1D, 1.5 nM of ConB induced a strong alkalinization of the phagosomal pH, reaching pH 8 (the higher limit of the FITC-based pH measure system used here) after 10 min of chase. In order to explore if such phagosomal alkalinization system was specific to DCs, we performed similar experiments using BMMO. Low (1.5 nM) ConB concentrations had no significant effect on phagosomal pH in

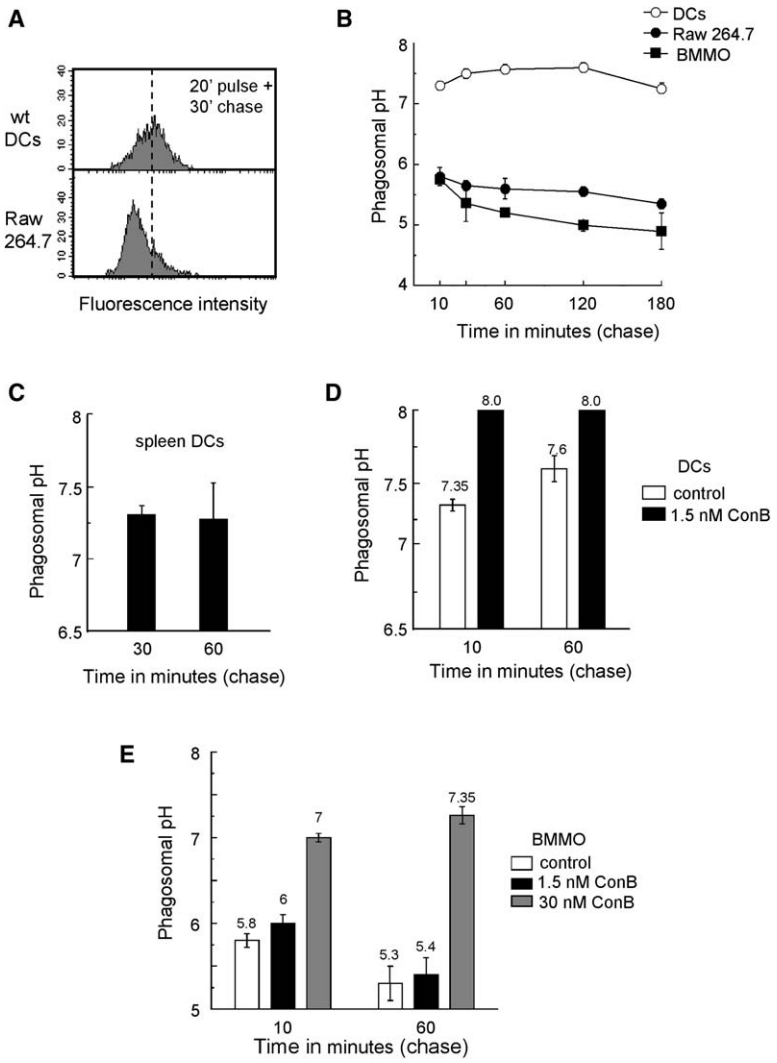

Figure 1. DCs Bear an Active System for Phagosomal Alkalinization

(A) Example of phagosomal pH analysis measured by FACS using FITC-coated latex beads.

(B) Kinetics of phagosomal pH after a 20 min phagocytosis pulse and the indicated times of chase.

(C) Phagosomal pH was measured in purified spleen DCs after a 20 min pulse with the beads and the different times of chase.

(D) Phagosomal pH in DCs at the indicated times in the presence or absence of 1.5 nM ConB. ConB induces a strong alkalinization of phagosomes. One of at least three independent experiments is shown.

(E) Effect of ConB (1.5 and 30 nM) on phagosomal pH in BMMO. ConB causes neutralization but not alkalinization of phagosomes. One of three independent experiments is shown.

macrophages, while high concentrations (30 nM) neutralized the phagosomal pH (from pH 5.3–5.8 to pH 7–7.35) (Figure 1E). As shown previously (Hackam et al., 1998; Yates and Russell, 2005), alkalinization of the phagosomal pH was observed in BMMO upon blockade of the V-ATPase.

We concluded that DCs and not macrophages bear an active machinery of phagosomal alkalinization, which maintains the phagosomal pH between 7 and 7.5 in the first few hours after phagocytosis. Upon inactivation of the V-ATPase, the phagosomal pH in DCs (but not in BMMO) alkalinizes strongly, showing that the V-ATPase is active, at least to some extent, in DC phagosomes.

NOX2 Recruitment and Activity in DC Phagosomes

In neutrophils, NOX2 generates ROS, which causes transient phagosome alkalinization, in part through the consumption of protons in the phagocytic lumen (Lee et al., 2003; Segal, 2005). We therefore hypothesized that ROS generation by NOX2 in DC phagosomes could be responsible for the active alkalinization of phagosomes in DCs. Since the intracellular localization of NOX2 transmembrane subunits in DCs has not been previously examined, we first analyzed the subcellular distribution of gp91*phox* using immunofluorescence and confocal microscopy. In resting DCs, gp91*phox* localizes to vesicular structures (Figure 2A) distributed throughout the cell, including dendrites, suggesting proximity with the plasma membrane. To investigate the morphology of gp91*phox*-positives structures, we analyzed the intracellular stores of cyt b558 using immunoelectron microscopy. Specific labeling of dense structures, similar to cyt b558-containing vesicles in neutrophils (Calafat et al., 1993), was often observed in the cell profiles (Figure 2B). When we analyzed the cells after 30 min of phagocytosis, cyt b558 was also visible in phagosomes (Figure 2C), indicating the recruitment of NOX2 to this compartment. To explore the recruitment of NOX2 to phagosomes more precisely, phagosomes were purified from wt and gp91*phox*-deficient DCs after different times of phagocytosis. DCs from

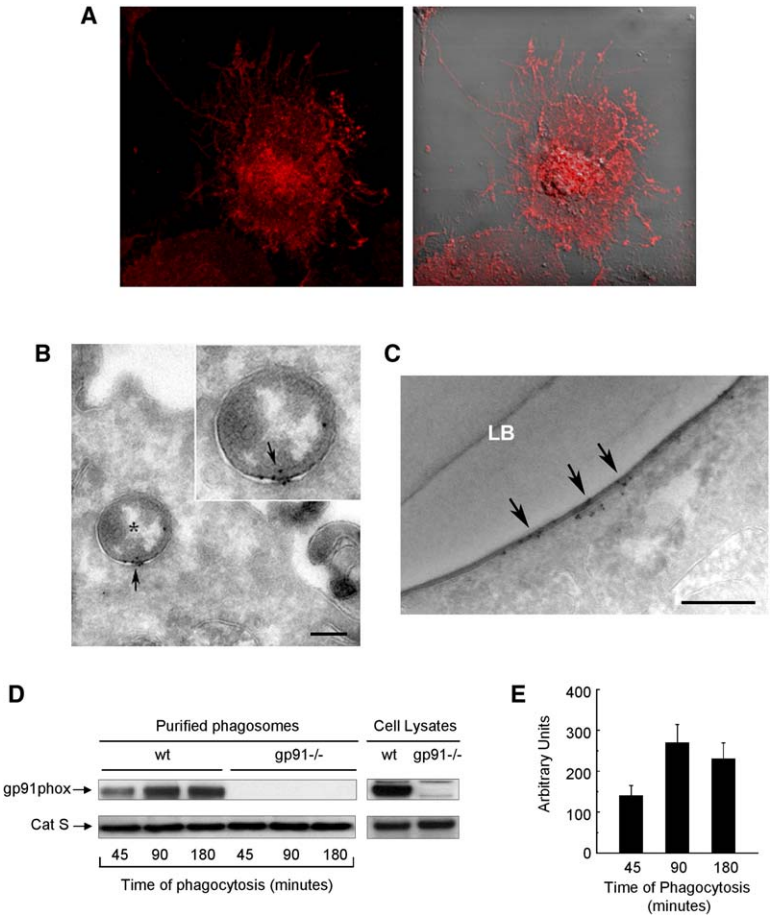

Figure 2. Recruitment of NOX2 to DC Phagosomes

(A) Immunofluorescence showing subcellular distribution of gp91*phox*-positive compartments in resting DCs.

(B) Ultrathin cryosections of wt DCs were immunogold labeled for cytochrome b558 (gp91*phox* and p22*phox*) (PAG 10). Membrane components of NOX2 were detected on electrondense compartments (arrows). The marked vesicle (asterisk) is shown at higher magnification in the inset. Bars: 200 nm.

(C) Cyt b558 recruitment to phagosomes was analyzed by immunoelectron microscopy; arrows show specific immunogold labeling (LB is latex bead).

(D) Magnetic bead phagosomes were purified from wt and gp91*phox*$^{-/-}$ (gp91$^{-/-}$) DCs as described in the Experimental Procedures. The kinetics of gp91*phox* recruitment to purified phagosomes was analyzed by Western blot. Catepsin S (Cat S) was used as a loading control. Analysis of the cell lysates (same experiment and Western blot) is shown in the right panels.

(E) Densitometry quantification of the Western blots of gp91*phox* from wt phagosomes from three independent experiments (average ± SEM).

gp91*phox*$^{-/-}$ mice developed normally, displayed a phenotype indistinguishable from that of wt (wild-type) DCs, and responded normally to LPS (Figure S2). Recruitment of the gp91*phox* to purified phagosomes was analyzed by Western blot. As shown in Figure 2D, gp91*phox* was recruited to phagosomes over time from wt DCs but not from gp91*phox*-deficient DCs. Quantification of the Western blots showed that the membrane components of NOX2 are effectively and rapidly recruited to DC phagosomes (Figure 2E).

We next attempted to determine if NOX2 was active in DC phagosomes. Activation of NOX2 implicates the recruitment of the cytosolic subunits such as p47*phox* to the membrane subunits (Cross and Segal, 2004). A clear label of the phagosomal membrane with anti-p47*phox* antibodies was evident after 1 hr of phagocytosis in wt DCs (Figure 3A, upper panels). A quantification of the fluorescence level around the phagosomes is depicted in Figure 3B. In gp91*phox*$^{-/-}$ DCs, no labeling of the phagosomes was observed, consistent with the known role of gp91*phox* in the membrane recruitment of p47*phox* (Figures 3A and 3B, lower panels). We conclude that NOX2 is effectively assembled on DC phagosomes only when gp91*phox* is present, suggesting that NOX2 is functional in this compartment in DCs.

DCs have previously been shown to produce low levels of ROS (Elsen et al., 2004; Matsue et al., 2003). To address the possible generation of ROS specifically in phagosomes, we covalently linked dihydrorhodamine 123 (DHR), a dye that only emits fluorescence under oxidative conditions, to latex beads (Vowells et al., 1995). As shown in Figures 3C (fluorescence microscopy) and 3D (FACS analysis), DHR-coated beads became fluorescent after phagocytosis, showing the production of ROS in DC phagosomes. This fluorescent signal was strongly inhibited by diphenylene iodonium (DPI), a specific inhibitor of flavin-containing enzymes such as NOX2. ROS production was not observed in phagosomes from gp91*phox*-deficient DCs. We conclude that the phagosomal environment in DCs is oxidative due to ROS generation by NOX2.

DCs Display Stronger and More Sustained Phagosomal NOX2 Activity Than BMMO

Like DCs, macrophages have been shown previously to produce ROS during phagocytosis or after activation (Forman and Torres, 2002). To compare ROS production over time in DCs and macrophages, we used a conventional luminol-based technique for ROS quantification. We first measured ROS production in DCs and BMMO treated with phorbol myristate acetate (PMA). PMA activates the

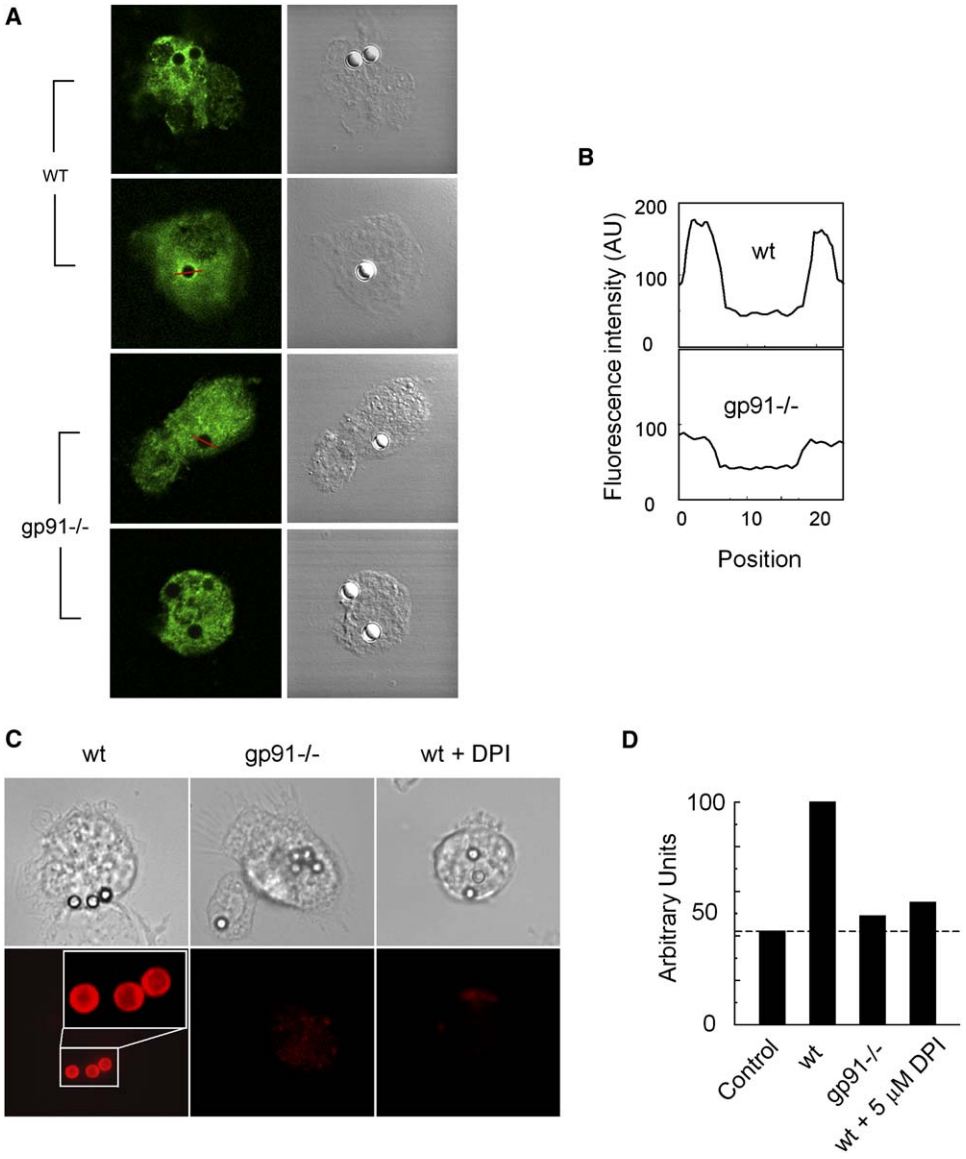

Figure 3. NOX2 Is Efficiently Assembled and Active in DC Phagosomes

(A) p47*phox* was detected by immunofluorescence and confocal microscopy in wt DCs (upper panels) and gp91*phox*$^{-/-}$ DCs (lower panels) after 60 min of phagocytosis.

(B) Quantifications of the fluorescence following the lines (depicted in A) in wt phagosome (upper panel) and gp91*phox*-deficient phagosome (lower panel).

(C) The cells were incubated with 3 μm beads coupled with dihydrorhodamine 123 (DHR) for a 15 min pulse and 45 min chase and immediately visualized by fluorescence microscopy.

(D) Phagosomal ROS measurement by FACS after 10 min of chase, as described in the Experimental Procedures. Data were normalized and expressed as arbitrary units. Dotted line indicates the autofluorescence signal.

protein kinase C, a potent activator of NOX2 (el Benna et al., 1994). ROS production in response to PMA was reproducibly higher and lasted longer in DCs than in macrophages (Figure 4A). In DCs, the inactivation was much slower, and significant ROS production was detected even after 2 hr of stimulation (Figure 4A). As expected, no ROS production was observed in gp91*phox*-deficient DCs (not shown). We concluded that the total capacity of ROS production is higher and NOX2 inactivation is slower in immature DCs than in BMMO. In order to evaluate ROS production selectively in phagosomes, we modified the classical technique used in Figure 4A by covalently attaching luminol to latex beads. ROS production in DC phagosomes was stronger and more sustained than in phagosomes from BMMO both in the absence (Figure 4B) and the presence of PMA (Figure 4C). In order

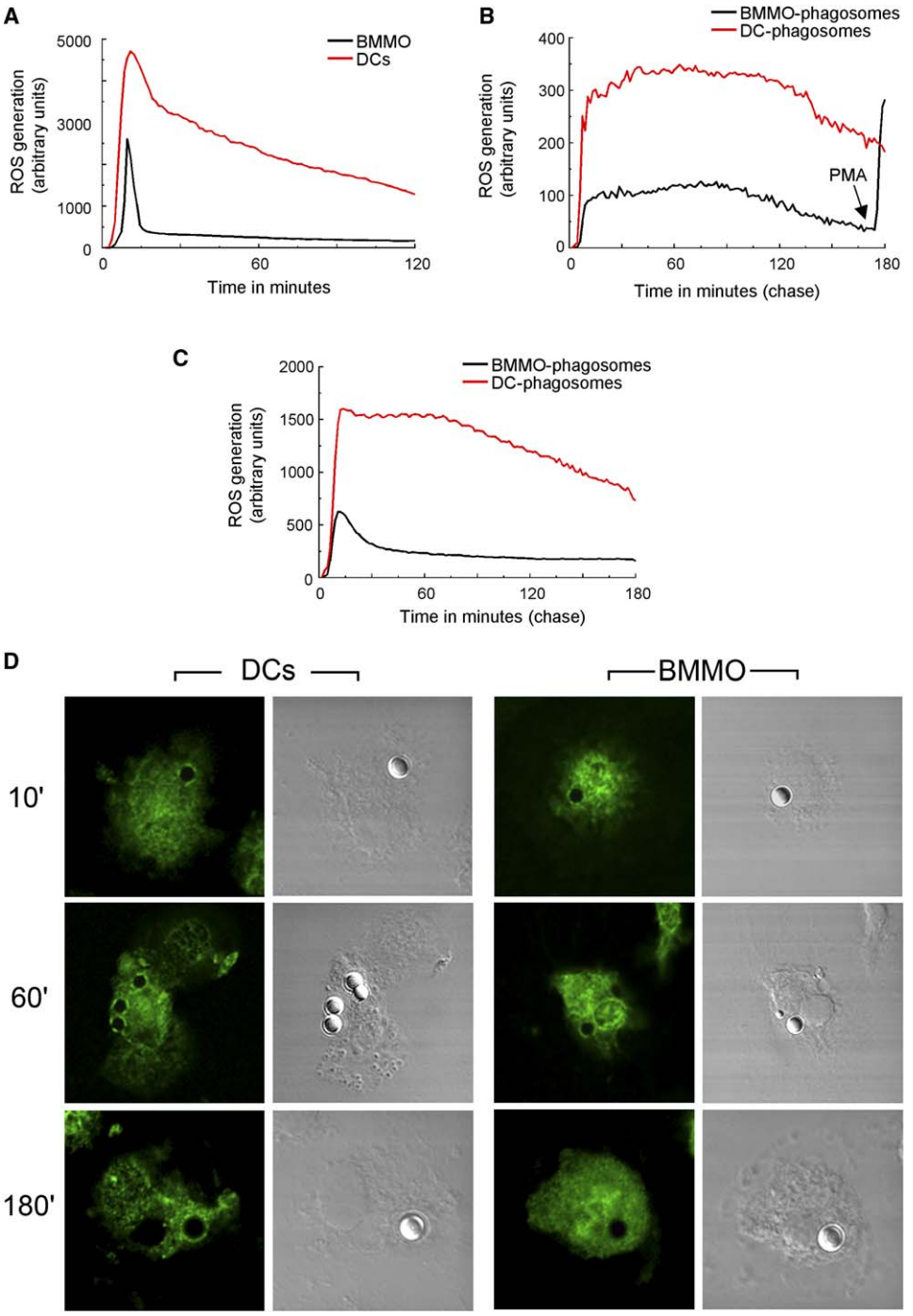

Figure 4. DCs Display More Efficient and Sustained NOX2 Activity Than BMMO

(A) Generation of ROS over time was measured using luminol-amplified chemiluminiscence after stimulation with 0.5 μg/ml PMA.

(B) After a 15 min pulse with luminol bound beads, the kinetics of NOX2 activity in phagosomes was evaluated. PMA was added to BMMO after 3 hr of phagocytosis to confirm that luminol on the beads was still active (arrow).

(C) Measurement of phagosomal ROS production using luminol bound beads (15 min pulse) when PMA was added at time 0 of chase. These results are representative of four independent experiments.

(D) Active assembly of NOX2 in phagosomes from DCs and BMMO was determined by p47*phox* immunofluorescence after 20 min pulse with latex beads and indicated times of chase. Cells were analyzed by confocal microscopy.

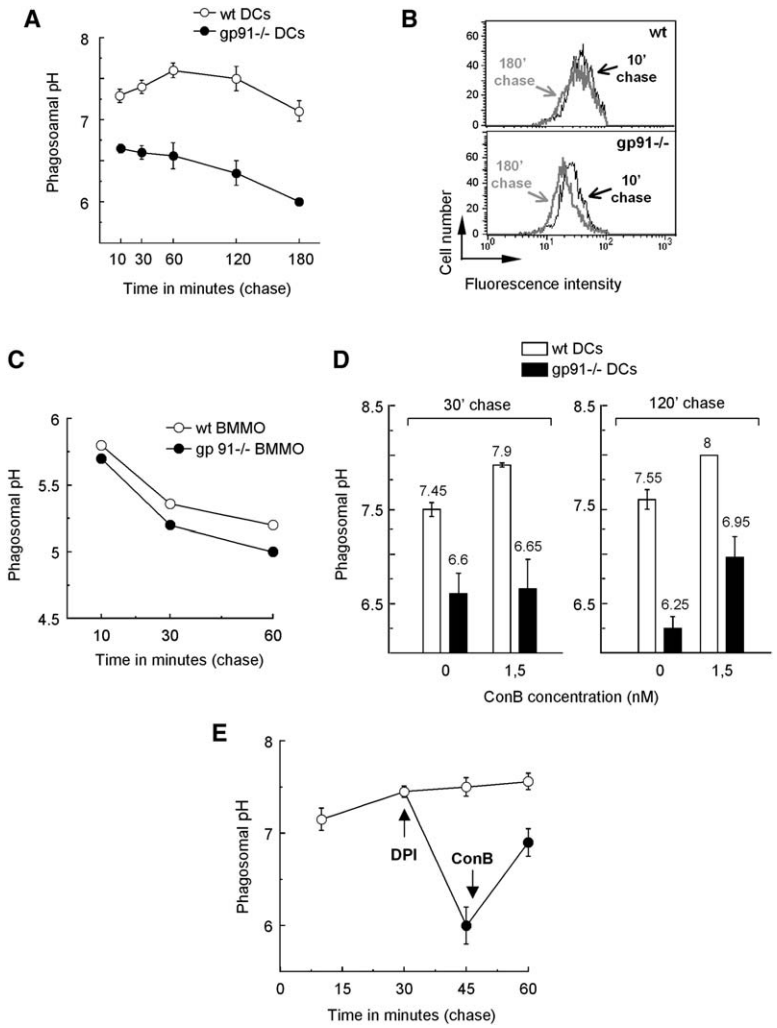

Figure 5. ROS Production in DC Phagosomes Causes Alkalinization of the Phagosomal Lumen

(A) Kinetics of phagosomal pH measurements after a 20 min phagocytosis pulse. Data and means ± SEM are from four independent experiments.

(B) Typical FACS profiles of the pH-sensitive dye for each cell type are shown after 10 min and 180 min of phagocytosis.

(C) Phagosomal pH measurement after 20 min pulse and indicated chase times in wt and gp91*phox*$^{-/-}$ BMMO.

(D) Measure of the phagosomal pH at 30 min or 120 min was performed in the presence or absence of 1.5 nM ConB. Data (± SEM) are representative of three independent experiments.

(E) pH in phagosomes was measured in wt DCs at 15 and 30 min of phagocytosis. After 30 min, DPI (10 μM) was added and the pH was analyzed 15 min later. At this time, ConB (1.5 nM) was added and the pH was measured 15 min later. All the results shown are representative of at least three experiments. Data and means ± SEM are from three independent experiments.

to exclude that BMMO degrade the luminol attached to the beads, thus preventing efficient ROS detection in phagosomes, PMA was added to macrophages after 3 hr of phagocytosis (Figure 4B, arrow).

The activation of NOX2 in phagosomes was also estimated through the analysis of the recruitment of p47*phox* to phagosomes using immunofluorescence and confocal microscopy. After 30 min of phagocytosis, effective NOX2 assembly on phagosomes was detected in both DCs and BMMO (Figure 4D). The fluorescent labeling of p47*phox* was more evident after 60 min of chase in both cell types. As shown in Figure 4D (lower panels), after 180 min of phagocytosis, however, only DC phagosomes maintained a clear labeling for p47*phox* (78% of DC phagosomes were visibly labeled, against 14% of BMMO phagosomes; at least 50 phagosomes analyzed in each case). We concluded that the sustained production of ROS in phagosomes from immature DCs is due to a prolonged assembly and activation of the NOX2 complex in DC phagosomes, as compared to BMMO phagosomes.

NOX2 Controls Alkalinization in DC Phagosomes

In order to test the possible involvement of NOX2 in the control of the phagosomal pH, we next measured phagosomal pH in gp91*phox* $^{-/-}$ DCs. The phagosomal pH was strongly decreased in gp91*phox*-defective DCs, as compared to wt DCs (Figures 5A and 5B), indicating that NOX2 activity controls pH in DC phagosomes. In contrast, wt and gp91*phox*-defective BMMO acidify their phagosomes with similar efficiencies (Figure 5C), indicating that the role of NOX2 in the control of phagosomal pH is restricted to DCs. Nevertheless, even in the absence of gp91*phox*, phagosome acidification in DCs was not as efficient as that observed in macrophages (in which the pH dropped to 5.2 in 60 min; see Figures 1B and 5C).

Upon blockade of the V-ATPase with ConB, the marked alkalinization observed in phagosomes from wt DCs was not observed in gp91*phox*-defective DCs (Figure 5D), showing that NOX2 mediates phagosome alkalinization in DCs. Surprisingly, neutralization of the phagosomal pH by ConB in the gp91*phox*-deficient DCs was observed only after 120 min, and not after 30 min of phagocytosis

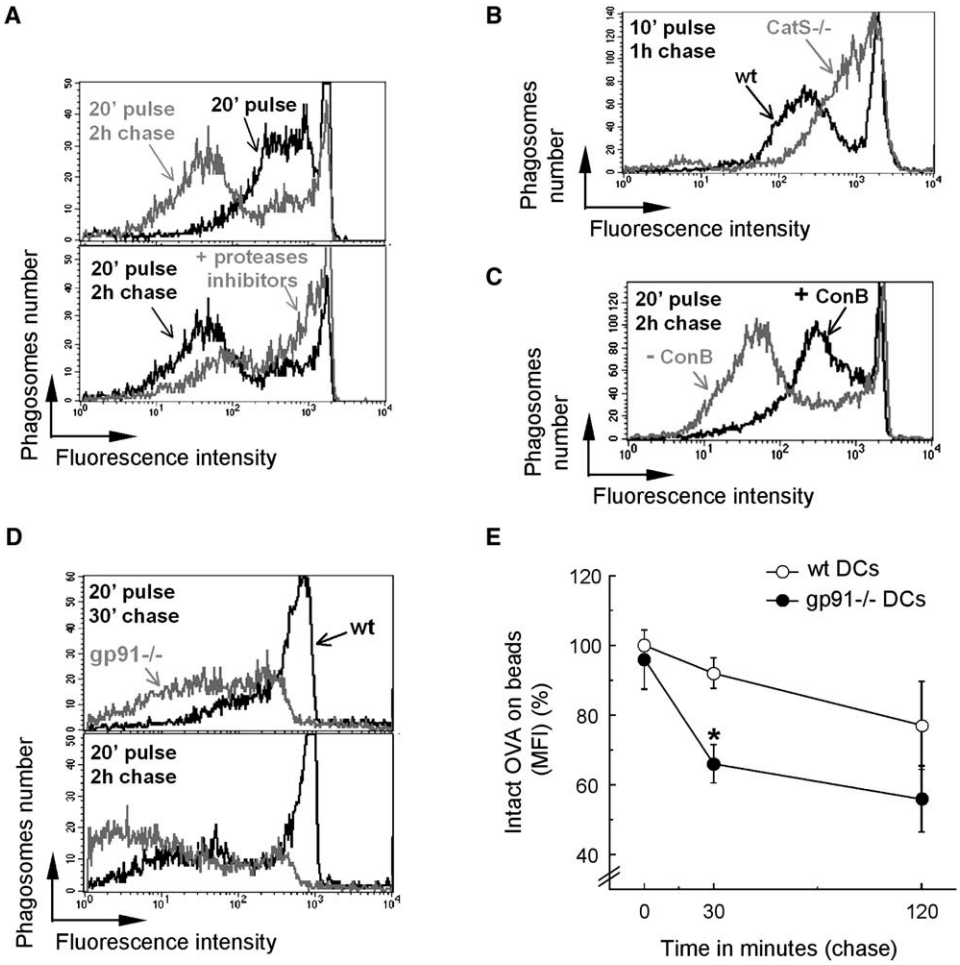

Figure 6. NOX2 Activity Limits Antigen Degradation in DC Phagosomes

(A) After different times of phagocytosis of OVA bound latex beads, the amount of OVA on the beads was quantified by FACS in the presence or absence of 1 mM of leupeptin/pepstatin.

(B) Same assay using phagosomes from wt or CatS$^{-/-}$ DCs.

(C) The experiment was also performed in the presence or absence of 20 nM ConB.

(D) Typical FACS profiles from one representative experiment showing the differences in phagosomal OVA degradation by wt and gp91$^{-/-}$-deficient cells at two different times of chase.

(E) Kinetics of OVA degradation in phagosomes from wt and gp91$^{-/-}$ DCs. Data and means ± SEM are from four independent experiments (*$p < 0.02$). The results are expressed as a percentage of the MFI obtained with wt DCs at time 0.

(Figure 5D), suggesting that in the long-term absence of NOX2 in phagosomes, other proton import pathways may become preeminent and mediate some degree of acidification. Indeed, when NOX2 was blocked at 30 min chase using DPI in wt DCs, the pH acidified within 15 min (Figure 5E). Upon inactivation of the V-ATPase by ConB, however, the pH increased in 15 min (Figure 5E), showing that in the absence of active NOX2, the V-ATPase still mediated acidification in DC phagosomes.

We conclude that NOX2 recruitment to DC phagosomes contributes to alkalinize the phagosomal lumen and maintains the pH above 7, in spite of the activity of the V-ATPase. In the absence of ROS generation in DC phagosomes (in the gp91*phox*-defective DCs or in the presence of DPI), the pH acidifies rapidly.

Antigen Degradation in gp91*phox*-Defective DCs

We next sought to evaluate the functional consequences of such a drop in phagosomal pH in terms of antigen degradation. To follow antigen degradation selectively in phagosomes, as opposed to all endocytic compartments, we set up a quantitative cytofluorometric assay for phagosomal degradation. After phagocytosis of beads covalently attached to OVA, the cells were lysed and the amount of OVA remaining on the beads was quantified using polyclonal OVA-specific antibodies and FACS analysis on the isolated beads. As shown in Figure 6A, a marked decrease over time in the amount of OVA attached to the beads was observed in wt DCs after 20 min pulse and 2 hr chase. This decrease was less pronounced in the presence of the protease inhibitors leupeptin and pepstatin (Figure 6A, lower

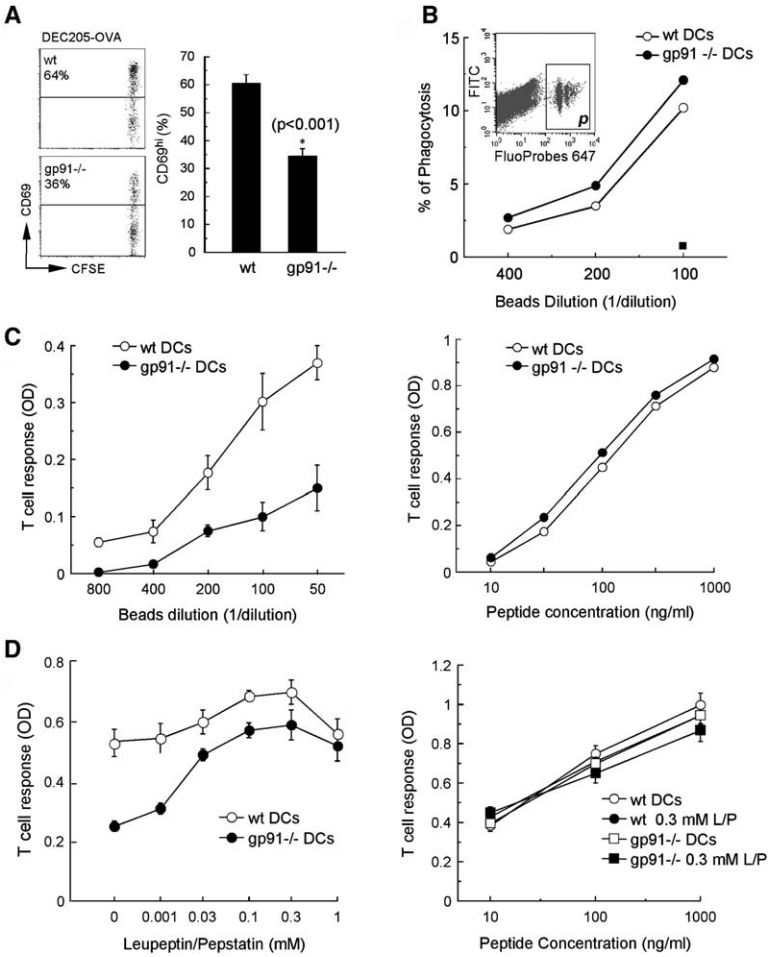

Figure 7. NOX2 Activity in DC Phagosomes Is Required for Crosspresentation

(A) In vivo crosspresentation is reduced in gp91*phox*-defective mice. Immunization of mice with αDEC205-OVA was performed as described in the Experimental Procedures. Representative FACS profiles of CD69 expression on CFSE positive populations are shown in the left panels. Results from three independent experiments are represented as mean ± SEM (right panel).

(B) Similar levels of phagocytosis in wt and gp91$^{-/-}$ DCs. After 1 hr of phagocytosis, the cells were analyzed by FACS (FCS/SSC population as shown in the inset). The percentage of cells having phagocytosed latex beads (region *p* in the inset) was calculated. A control at 4°C was performed to estimate the percentage of bead association to DCs (square symbol).

(C) In vitro crosspresentation of OVA coated beads by wt and gp91*phox*$^{-/-}$ DCs (left panel) or OVA peptide (right panel) was assayed as described in Experimental Procedures.

(D) Crosspresentation of OVA beads (1:200) was assayed as before in the presence of increasing concentrations of leupeptin/pepstantin (left panel). A control with OVA peptide was done in the presence or not of 0.3 mM of leupeptin/pepstatin (right panel). The results shown (C) and (D) (mean ± SEM) are representative of at least three experiments.

panel) or in DC phagosomes from Cathepsin S (Cat S)-deficient mice (Figure 6B). We conclude that decreased immunofluorescence on the beads was due to actual degradation rather than denaturation of OVA.

As shown in Figure 6C, ConB induced a marked inhibition of OVA degradation, showing that the lysosomal proteases present in phagosomes are more active at pH 7–7.5 (the pH in control DCs) than at pH 7.5–8 (the pH in ConB-treated DCs; see Figure 1D). On the contrary, in gp91*phox*-deficient DCs, in which the phagosomal pH is more acidic than in wt DCs (see Figure 5), the degradation of bead bound OVA was accelerated as compared to wt DCs, as shown in fluorescence intensity histograms from one representative experiment after 30 and 120 min of chase (Figure 6D). Over five independent experiments, the acceleration of OVA degradation in DCs from gp91*phox*-deficient mice, as compared to wt DCs, was most evident after 30 min of chase (Figure 6E). We conclude that NOX2 activity in DC phagosomes limits antigen degradation.

NOX2 Is Required for Efficient Antigen Crosspresentation by DCs

To examine if excessive acidification and antigen degradation in phagosomes affected antigen presentation, we first evaluated cross priming of adoptively transferred OVA-specific, CD8$^+$ OT-1 cells into wt and gp91*phox*$^{-/-}$ mice after selective targeting of OVA to resident DCs (using OVA coupled to anti-DEC205 antibodies [Bonifaz et al., 2002]). As shown in Figure 7A, OT-1 activation was less efficient in gp91*phox*-defective mice than in wt mice ($p < 0.001$), suggesting that the efficiency of crosspresentation of OVA by DCs in vivo is decreased in the absence of NOX2.

To test this possibility more directly, the efficiency of antigen crosspresentation in wt and gp91*phox*-defective DCs was measured in vitro. Because crosspresentation requires antigen uptake, we first evaluated the efficiency of endocytosis (not shown) and phagocytosis in gp91*phox*-defective DCs. Phagocytosis was measured by FACS after a 20 min pulse and a 60 min chase with different concentrations of fluorescent latex beads. The percentage of DCs having phagocytosed at least one latex bead (area *p* in the inset of Figure 7, panel B) was similar in gp91*phox*-deficient and wt DCs (Figure 7B).

As shown in the left panel of Figure 7C, gp91*phox*-defective DCs failed to crosspresent OVA efficiently (a 4- to 6-fold increase in the concentration of OVA required, as compared to wt). The presentation of the

corresponding OVA peptide (SIINFEKL, i.e., the peptide already processed) was similar in both DCs populations, showing that DCs from gp91*phox*$^{-/-}$ mice are fully competent for T cell activation (Figure 7C, right panel). This result indicates that the defect in crosspresentation observed in gp91*phox*$^{-/-}$-deficient DCs is related to antigen processing and not to antigen presentation per se. Inhibition of oxidase activity by DPI also strongly inhibited OVA crosspresentation in wt DCs (Figure S3, left panel) without any effect on the presentation of the peptide (Figure S3, right panel). The requirement for NOX2 activity for antigen processing in crosspresentation was not restricted to OVA since crosspresentation of a long HY peptide to TCR transgenic CD8$^+$ HY-specific Mata Hari T cells was also inefficient in gp91*phox*$^{-/-}$ DCs (Figure S4). We conclude that NOX2 activity in DCs is required to crosspresent OVA and HY antigens efficiently to CD8$^+$ T cells.

Thus, DCs from gp91*phox*-defective mice have increased antigen degradation and inefficient antigen crosspresentation, suggesting that decreased crosspresentation in gp91*phox*$^{-/-}$ DCs was due to excessive phagosomal degradation. To address this possibility, wt and gp91*phox*$^{-/-}$ DCs were treated with increasing concentrations of protease inhibitors (a mix of leupeptin and pepstatin) in order to partially inhibit degradation in phagosomes. As shown in the left panel of Figure 7D, at low protease inhibitor concentrations, crosspresentation of OVA in gp91-defective DCs was increased, reaching wt levels. Treatment of the DCs with protease inhibitors did not affect peptide presentation to the same T cell hybrid (Figure 7D, right panel). Therefore, partial inhibition of proteolysis in gp91*phox*-defective DCs overcomes the crosspresentation defect, indicating that excessive antigen degradation in phagosomes from gp91*phox*-defective DCs, resulting from abnormal acidic pH, is the cause of inefficient crosspresentation.

DISCUSSION

Our results have revealed a novel mode of regulation of phagosome acidification and proteolysis in DCs: the recruitment of NOX2 to phagosomes mediates a sustained production of ROS, which results in proton consumption in the phagosome lumen, causing the pH to rise to 7.4 ± 0.2, in spite of the presence of active V-ATPase. Thus, the phagosomal pH in DCs is controlled by the respective activities of two large molecular complexes: one that imports protons across the phagosomal membrane (the V-ATPase), and NOX2, which causes proton consumption in the phagosomal lumen (after dismutation of peroxide anions into hydrogen peroxide). Depending on the recruitment and level of activity of these two large molecular complexes to DC phagosomes, the pH alkalinizes or acidifies.

A role for NOX2, a major player of innate immune responses in neutrophils, in the regulation of adaptative immunity (through the control of antigen presentation in DCs) is certainly a surprise. The expression of NOX2 in DCs, however, was shown in previous studies (Elsen et al., 2004; Matsue et al., 2003; Vulcano et al., 2004) in which ROS generation was referred to as "cryptic" (as it represented 2%–5% of that found in neutrophils). In neutrophils, the generation of ROS by NOX2 influences the phagosomal pH through different pathways, including the mobilization of certain ions (such as K^+) and proton consumption upon dismutation of ROS in the lumen of phagosomes, causing transient and strong alkalinization (Reeves et al., 2002), consistent with a rapid and transitory activation of NOX2 (Segal and Coade, 1978). After the first few minutes of respiratory burst, however, the phagosomal pH acidifies very rapidly (Segal, 2005; Segal et al., 1981). In macrophages, the kinetics of NOX2 activation and inactivation were similar to those observed in neutrophils but did not influence phagosomal pH, most likely due to the low levels of ROS production as compared to the high activity of the V-ATPase. In DCs, in contrast, sustained production of ROS was observed for several hours. Combined with the low activity of the V-ATPase (Trombetta et al., 2003), ROS production resulted in the sustained alkalinization of the phagosomal lumen. The regulation of the pH in DC phagosomes would therefore result from a delicate balance between the electrogenic activity of NOX2, which causes proton consumption in the phagosome lumen, and the translocation of protons from the cytosol mediated by the V-ATPase and other proton permeable channels (DeCoursey et al., 2001; DeCoursey et al., 2003; Nanda et al., 1994).

It was quite surprising, however, that the effect of ConB on phagosomal pH was more dramatic (and rapid) in wt DCs treated with DPI (neutralization of the phagosomal pH in 15 min), than in gp91*phox*-deficient DCs, in which we only observed neutralization of the phagosomal pH after 2 hr of treatment (see Figures 5D and 5E). This difference in the effect of ConB in the two situations suggests that long-term defect in NOX2 activity may cause certain adaptations of proton transport in endosomes and phagosomes. The relative resistance to ConB in the gp91*phox*-deficient DCs could be due to a decreased recruitment of the V-ATPase to gp91$^{-/-}$ phagosomes or to the development of alternative proton transfer routes (DeCoursey et al., 2001, 2003; Nanda et al., 1994). In any case, ConB did neutralize the phagosomal pH when NOX2 was inactive, establishing that the enhanced acidification in the absence of active NOX2 was indeed due to the V-ATPase. In addition, the inhibition of crosspresentation by DPI in wt DCs was much stronger (Figure S3) than gp91*phox*$^{-/-}$ DCs. Consistently, phagosome acidification in DPI-treated cells was more efficient than in gp91*phox*-deficient cells, suggesting again that gp91*phox*-deficient cells have somehow "adapted" to the NOX2 defect to limit phagosome acidification.

The idea that exacerbated antigen degradation is detrimental to antigen presentation to T cells was proposed by others (Accapezzato et al., 2005; Delamarre et al., 2005). Our results provide the first genetic evidence supporting this idea and identify one of the underlying mechanisms

that limit acidification in DCs, as compared to macrophages. We would therefore like to propose that the phagosomal pH in phagocytic cells determines if this compartment is more adapted to "kill" or "process." Acidification in macrophages is extremely efficient, aiming at maximal lysosomal protease activity and microbe killing. In contrast, antigen processing requires a delicate equilibrium between "some" degradation (to generate antigenic peptides) and "not too much" degradation (which could destroy potential T cell epitopes).

Although our results are based on the analysis of a few model antigens, OVA and HY, we may have unraveled a general mechanism of control of proteolysis in DC phagosomes and thereby of antigen processing in DCs. Indeed, our preliminary results show that MHC class II-restricted presentation of OVA and HY to $CD4^+$ T cells by DCs is also defective in gp91$^{-/-}$ DCs (our unpublished data). It is most likely that depending on the resistance or sensitivity of antigens to different proteases and on the structure of particular epitopes, the effect of excessive degradation on antigen presentation might be more or less pronounced. pHs above 7 (the natural pHs in DC phagosomes) are favorable for crosspresentation, suggesting that the proteolytic enzymes detrimental for crosspresentation of OVA and HY are inactive at these pHs. Consequently, proteolytic enzymes with optimal pH around 7, such as CatS or furin (Claus et al., 1998), are probably not the ones that inhibit antigen crosspresentation. In contrast, when the pH in phagosomes was lower than 6.5 (in gp91*phox*$^{-/-}$ DCs or in DPI-treated DCs), antigen presentation was inefficient, suggesting that proteases with optimal pH values around or below 6.5 (which should be more active at pH 6.5 than at pH 7.5) could prevent efficient crosspresentation. Proteases with such characteristics include cathepsins B, L, and H, as well as AEP (Claus et al., 1998; Manoury et al., 1998). Consistent with this possibility, low concentrations of leupeptin/pepstatin, conventional inhibitors of cystein proteases, partially inhibited OVA degradation and restored crosspresentation in gp91*phox*-defective DCs.

Altogether, our results show that a major player of innate immune responses, NOX2, is also involved in the control of adaptative immunity. Defects in NOX2 cause chronic granulomatosis disease, a genetic immunodeficiency resulting from a defect in neutrophils-mediated innate defenses against pathogenic bacteria. It would be interesting, although not very easy because of repetitive infections in these patients, to evaluate DCs function and adaptative immune responses in this disease.

EXPERIMENTAL PROCEDURES

Cells

Primary cultures of immature DCs were generated by 7–15 days of culture of bone marrow cells in granulocyte-macrophage colony stimulating factor-containing medium, as previously described (Winzler et al., 1997). Maturation was induced by 16 hr treatment with 10 μg/ml of lipopolysachharides (LPS). BMMO were generated by 7 days of culture of bone marrow cells in macrophage colony stimulating factor (M-CSF).

Crosspresentation Assays

Crosspresentation was assayed as described previously (Guermonprez et al., 2003). OVA was attached to 3 μm latex beads by passive adsorption in PBS at 4°C, and extensive washes in PBS. DCs were allowed to phagocytose OVA beads, and BSA beads for the indicated times. Alternately, DCs were loaded with the specific OVA peptide as a control of surface exposure of MHC class I molecules. Then cells were fixed with 1% paraformaldehyde in 96 flat-well plates, washed, and cultured for 18 hr with the B3Z, $CD8^+$ T cell hybridoma cells (Karttunen et al., 1992). B3Z activation was monitored as described in Karttunen et al. (1992).

Phagocytosis Measurement by FACS Analysis

Phagocytosis was determined using beads coupled with FITC and FluoProbes647. Cells were incubated for 1 hr at 37°C in the presence of increasing dilutions of fluorescent beads. The cells were then extensively washed with cold PBS and immediately analyzed by FACS. The percentage of phagocyting cells was calculated. A control at 4°C with the maximal concentration of beads was done to calculate the proportion of beads that are associated with but not phagocytosed by DCs.

Phagosomes Purification

DCs were incubated at indicated times with 3 μm magnetic latex beads and then disrupted in Homogenization Buffer as described (Guermonprez et al., 2003). Magnetic phagosomes were removed from the postnuclear supernatant using a magnet, washed three times in cold PBS, and lysed. After 15 min at 4°C, the magnetic beads were removed.

Phagosomal Protein Degradation Assay

OVA (0.5 mg/ml) was covalently coupled after activation of 3 μm latex beads with glutharaldehyde 8%, according to manufacturer's directions. DCs were pulsed and chased at the indicated times with the coupled latex beads. Cells were disrupted in lysis buffer and centrifuged at 900 rpm for 4 min at 4°C. Supernatants containing the latex beads were collected and stained with a rabbit polyclonal anti-OVA antibody and FITC-coupled anti-rabbit antibodies in 96 well conic-bottom microplates. The beads were then analyzed by FACS.

Measurement of Phagosomal pH

Three micrometers of polybeads amino were covalently coupled with FITC (pH sensitive) and FluoProbes 647 (pH insensitive) in the presence of sodium hydrogen carbonate buffer at pH 8 for 2 hr at room temperature. After extensively washing with glycine 100 mM, the beads were suspended in PBS. The cells were pulsed with the coupled beads for 20 min and then extensively washed in cold PBS. The cells were then incubated at 37°C ("chased") for the indicated times and immediately analyzed by FACS, using a gating FCS/SSC selective for cells that have phagocytosed one latex bead. The ratio of the mean fluorescence intensity (MFI) emission between the two dyes was determined. Values were compared with a standard curve obtained by resuspending the cells that had phagocytosed beads for 2 hr at a fixed pH (ranging from pH 5.5 to 8) and containing 0.1% Triton X100. The cells were immediately analyzed by FACS to determine the emission ratio of the two fluorescent probes at each pH. To certify that the decrease in FITC fluorescence observed at low pH was not due to loss of FITC from the beads, the pH 5.5 buffer was neutralized after measurement using OHNa (see Figure S1B). In some cases, DCs or BMMO were incubated for 20 min before pulse with the indicated concentrations of the drug (ConB). To evaluate the effect of blocking NOX2 activity, 10 μM of DPI was added to wt DCs after 30 min chase, and phagosomal pH was measured 15 min later. Then, ConB was added, and a new pH measurement was performed 15 min later.

Analysis of Phagosomal NOX2 Activity

Detection of ROS Using a Fluorescent Probe

Three micrometers of polybeads amino were covalently coupled with DHR and FluoProbes 647 in the presence of sodium hydrogen

carbonate buffer at pH 8 for 2 hr at room temperature. After extensively washing with glycine 100 mM, beads were resuspended in PBS. DCs were pulsed with the DHR-coupled beads during 20 min and then extensively washed in cold PBS. After incubation with the beads, the cells were chased for the indicated times and immediately analyzed by FACS using a FCS/SSC gating selective for cells that have phagocytosed one latex bead. The variation of the MFI emission of DHR was determined. For DPI assay, cells were incubated in the presence of 5 μM DPI for 30 min before and during the 20 min pulse. Alternatively, a fluorescent microscopy assay was performed. DCs were pulsed with beads coupled covalently with DHR (dilution of 1:100) for 20 min. After extensive washing with cold PBS, cells were chased for 45 min and immediately analyzed by inverted fluorescence microscopy (Leica DMI6000 B).

Measurement of NOX2 Activity by Chemiluminiscence

DCs and BMMO (3×10^6 cells) were resuspended in 300 μl of CO_2-independent medium containing 10 μM luminol (the probe that releases energy as visible light upon oxidation) and five units of horseradish peroxidase. Cell suspensions were preheated to 37°C in the thermostated chamber of the luminometer (Berthold-Biolumat LB937) and allowed to stabilize. Then, they were stimulated with 0.5 μg/ml PMA, and changes in chemiluminiscence were measured over the indicated times. For phagosomal measurements, luminol was covalently coupled to 3 μm polybeads amino after activation with glutharaldehyde 8%, according to manufacturer's directions. DCs and BMMO were pulsed with luminol bound beads for 15 min and then extensively washed with glycine 100 mM and resuspended in PBS. In order to obtain similar percentages of cells having phagocytosed beads, the dilution of beads used during the pulse was slightly higher with macrophages than with DCs. The percentage of phagocytosis in the experiment shown in Figure 4 was 12.7% in DCs and 13.4% in macrophages. Cells were resuspended in 300 μM of CO_2-independent medium containing five units of horseradish peroxidase and placed in the luminometer at 37°C for chemiluminiscence measurement over 180 min. Alternatively, 0.5 μg/ml PMA was added to DCs and BMMO just before starting the measurements.

Immunofluorescence Assay

wt DCs were plated on poly-L-lysine-coated glass coverslips (12 mm) for 10 min at room temperature (RT). The coverslips were washed, and complete medium was added to further incubate the attached cells at 37°C and 5% CO_2 for 45 min. The cells were then washed and fixed in 2% paraformaldehyde (PFA) for 10 min at RT. After two washes with 1 mM glycine PBS, cells were permeabilized and incubated with antibodies in PBS plus 0.2% BSA plus 0.05% saponin for 1 hr (primary antibodies, dilution of 1:300). Bound antibodies were subsequently detected by incubation with fluorescent conjugated secondary antibody for 45 min. After washes, the coverslips were mounted on glass slides using fluoromount G. For p47*phox* labeling, DCs were placed on poly-L-lysine-coated coverslips at 37°C in an atmosphere of 5% CO_2 during a short period. Attached cells were pulsed with beads (dilution of 1:500) during 20 min and extensively washed with cold PBS. Completed medium was added and cells were chased for 40 min. After washing, the cells were fixed and treated as described before for immunolabeling. Alternatively, a pulse of 15 min with latex beads, followed by extensive washing of DCs and BMMO before incubation on poly-L-lysine-coated glass coverslips. Complete medium was added and chases of 10, 60, or 180 min were done at 37°C and an atmosphere of 5% CO_2 before fixation. Immunofluorescence images were acquired with Zeiss confocal microscope (LSM Axivert 720) using 63 × 1.4 NA oil immersion objective. Fluorescence intensity around phagosomes from confocal images was analyzed by Metamorph 6.3.

In Vivo Crosspresentation Assay

$CD8^+$ T cells from OT-1 T cell receptor (TCR) transgenic mice were labeled with carboxyfluorescein succinimidyl ester (CFSE) (2 μM) and 2×10^6 cells were transferred into 4- to 5-week-old female gp91*phox* $^{-/-}$ and homozygous wt recipients by injection into the tail vein. Then, recipient mice were injected subcutaneously with 0.1 μg of αDEC205-OVA per footpad. For monitoring T cell activation, CD69 expression on CFSE positive cells and OT-1 cells was measured by FACS 18 hr later.

αDEC205-OVA conjugates were produced and purified as described (Bonifaz et al., 2002). Live animal experiments were in accordance to the guidelines of the French Veterinary Department.

Electron Microscopy

DCs from C57BL/6 wt mice were used for phagocytosis experiments and fixed with a mixture of 2% paraformaldehyde and 0.125% glutaraldehyde in 0.2 M phosphate buffer with a pH of 7.4 for 2 hr at room temperature. Fixed cells were processed for ultrathin cryosectioning, immunogold labeled, and contrasted as described previously (Raposo et al., 1997).

Immunoblotting

Protein extracts (2 μg/lane) from purified phagosomes were subjected to SDS-PAGE on 4%–12% gradient gel. After transferring, the membranes were blocked and incubated with primary antibodies and peroxidase-conjugated secondary antibodies. Bound antibodies were revealed using the Supersignal West Pico Chemiluminescent Substrate or with a kit from Roche according to the manufacturers' directions. The intensity of the bands was quantified by densitometry and was expressed as arbitrary units.

Supplemental Data

Supplemental Data include nine figures and four tables and can be found with this article online at http://www.cell.com/cgi/content/full/126/1/205/DC1/.

ACKNOWLEDGMENTS

We are especially grateful to Azzaq Belaaouaj (University of Reims), Michel Mallat (Hôpital de la Salpêtriere, Paris), Gaetan Gavazzi, and Karl-Heinz Krause (University of Geneva) for the gp91*phox*-deficient mice. We thank Jero Calafat and Hans Janssen (The Netherlands Cancer Institut) for the gift of 7D5 antibody (anti-cyt b558), Jamel el Benna (Xavier Bichat Hospital, Paris) for useful discussion and providing the anti-gp91*phox* and anti-p47*phox* antibodies, Olivier Lantz (Institut Curie), Matthew Albert (Institut Pasteur) and Hansjörg Schild (Mainz) for HY long peptide design and validation, Philippe Benaroch for helpful discussions and providing ConB. We also acknowledge Andres Floto, Jorge Geffner, Ira Mellman, and Vincenzo Barnaba for useful discussions and Alexandre Boissonnas for assistance with the in vivo experiments. We are grateful to the Ligue National de Lutte Contre le Cancer, DC-THERA (LSHG-CT-2004-512074), the Welcome Trust, and BBSRC for support. A.S. was supported by LLNC, INSERM, and Marie Curie Fellowship Program.

Received: December 1, 2005
Revised: March 10, 2006
Accepted: May 3, 2006
Published: July 13, 2006

REFERENCES

Accapezzato, D., Visco, V., Francavilla, V., Molette, C., Donato, T., Paroli, M., Mondelli, M.U., Doria, M., Torrisi, M.R., and Barnaba, V. (2005). Chloroquine enhances human CD8+ T cell responses against soluble antigens in vivo. J. Exp. Med. *202*, 817–828.

Banchereau, J., and Steinman, R.M. (1998). Dendritic cells and the control of immunity. Nature *392*, 245–252.

Benaroch, P., Yilla, M., Raposo, G., Ito, K., Miwa, K., Geuze, H.J., and Ploegh, H.L. (1995). How MHC class II molecules reach the endocytic pathway. EMBO J. *14*, 37–49.

Bonifaz, L., Bonnyay, D., Mahnke, K., Rivera, M., Nussenzweig, M.C., and Steinman, R.M. (2002). Efficient targeting of protein antigen to the dendritic cell receptor DEC-205 in the steady state leads to antigen presentation on major histocompatibility complex class I products and peripheral CD8+ T cell tolerance. J. Exp. Med. *196*, 1627–1638.

Calafat, J., Kuijpers, T.W., Janssen, H., Borregaard, N., Verhoeven, A.J., and Roos, D. (1993). Evidence for small intracellular vesicles in human blood phagocytes containing cytochrome b558 and the adhesion molecule CD11b/CD18. Blood *81*, 3122–3129.

Claus, V., Jahraus, A., Tjelle, T., Berg, T., Kirschke, H., Faulstich, H., and Griffiths, G. (1998). Lysosomal enzyme trafficking between phagosomes, endosomes, and lysosomes in J774 macrophages. Enrichment of cathepsin H in early endosomes. J. Biol. Chem. *273*, 9842–9851.

Cresswell, P. (2005). Antigen processing and presentation. Immunol. Rev. *207*, 5–7.

Cross, A.R., and Segal, A.W. (2004). The NADPH oxidase of professional phagocytes-prototype of the NOX electron transport chain systems. Biochim. Biophys. Acta *1654*, 1–22.

DeCoursey, T.E., Cherny, V.V., Morgan, D., Katz, B.Z., and Dinauer, M.C. (2001). The gp91phox component of NADPH oxidase is not the voltage-gated proton channel in phagocytes, but it helps. J. Biol. Chem. *276*, 36063–36066.

DeCoursey, T.E., Morgan, D., and Cherny, V.V. (2003). The voltage dependence of NADPH oxidase reveals why phagocytes need proton channels. Nature *422*, 531–534.

Delamarre, L., Pack, M., Chang, H., Mellman, I., and Trombetta, E.S. (2005). Differential lysosomal proteolysis in antigen-presenting cells determines antigen fate. Science *307*, 1630–1634.

el Benna, J., Faust, L.P., and Babior, B.M. (1994). The phosphorylation of the respiratory burst oxidase component p47phox during neutrophil activation. Phosphorylation of sites recognized by protein kinase C and by proline-directed kinases. J. Biol. Chem. *269*, 23431–23436.

El-Benna, J., Dang, P.M., Gougerot-Pocidalo, M.A., and Elbim, C. (2005). Phagocyte NADPH oxidase: a multicomponent enzyme essential for host defenses. Arch. Immunol. Ther. Exp. (Warsz.) *53*, 199–206.

Elsen, S., Doussiere, J., Villiers, C.L., Faure, M., Berthier, R., Papaioannou, A., Grandvaux, N., Marche, P.N., and Vignais, P.V. (2004). Cryptic O2- -generating NADPH oxidase in dendritic cells. J. Cell Sci. *117*, 2215–2226.

Forman, H.J., and Torres, M. (2002). Reactive oxygen species and cell signaling: respiratory burst in macrophage signaling. Am. J. Respir. Crit. Care Med. *166*, S4–S8.

Guermonprez, P., Valladeau, J., Zitvogel, L., Thery, C., and Amigorena, S. (2002). Antigen presentation and T cell stimulation by dendritic cells. Annu. Rev. Immunol. *20*, 621–667.

Guermonprez, P., Saveanu, L., Kleijmeer, M., Davoust, J., Van Endert, P., and Amigorena, S. (2003). ER-phagosome fusion defines an MHC class I cross-presentation compartment in dendritic cells. Nature *425*, 397–402.

Guermonprez, P., and Amigorena, S. (2005). Pathways for antigen crosspresentation. Springer Semin. Immunopathol. *26*, 257–271.

Hackam, D.J., Rotstein, O.D., Zhang, W., Gruenheid, S., Gros, P., and Grinstein, S. (1998). Host resistance to intracellular infection: mutation of natural resistance-associated macrophage protein 1 (Nramp1) impairs phagosomal acidification. J. Exp. Med. *188*, 351–364.

Heath, W.R., Belz, G.T., Behrens, G.M., Smith, C.M., Forehan, S.P., Parish, I.A., Davey, G.M., Wilson, N.S., Carbone, F.R., and Villadangos, J.A. (2004). Cross-presentation, dendritic cell subsets, and the generation of immunity to cellular antigens. Immunol. Rev. *199*, 9–26.

Houde, M., Bertholet, S., Gagnon, E., Brunet, S., Goyette, G., Laplante, A., Princiotta, M.F., Thibault, P., Sacks, D., and Desjardins, M. (2003). Phagosomes are competent organelles for antigen cross-presentation. Nature *425*, 402–406.

Jiang, Q., Griffin, D.A., Barofsky, D.F., and Hurst, J.K. (1997). Intraphagosomal chlorination dynamics and yields determined using unique fluorescent bacterial mimics. Chem. Res. Toxicol. *10*, 1080–1089.

Karttunen, J., Sanderson, S., and Shastri, N. (1992). Detection of rare antigen-presenting cells by the lacZ T-cell activation assay suggests an expression cloning strategy for T-cell antigens. Proc. Natl. Acad. Sci. USA *89*, 6020–6024.

Kjeken, R., Egeberg, M., Habermann, A., Kuehnel, M., Peyron, P., Floetenmeyer, M., Walther, P., Jahraus, A., Defacque, H., Kuznetsov, S.A., and Griffiths, G. (2004). Fusion between phagosomes, early and late endosomes: a role for actin in fusion between late, but not early endocytic organelles. Mol. Biol. Cell *15*, 345–358.

Lee, W.L., Harrison, R.E., and Grinstein, S. (2003). Phagocytosis by neutrophils. Microbes Infect. *5*, 1299–1306.

Lennon-Dumenil, A.M., Bakker, A.H., Maehr, R., Fiebiger, E., Overkleeft, H.S., Rosemblatt, M., Ploegh, H.L., and Lagaudriere-Gesbert, C. (2002). Analysis of protease activity in live antigen-presenting cells shows regulation of the phagosomal proteolytic contents during dendritic cell activation. J. Exp. Med. *196*, 529–540.

Manoury, B., Hewitt, E.W., Morrice, N., Dando, P.M., Barrett, A.J., and Watts, C. (1998). An asparaginyl endopeptidase processes a microbial antigen for class II MHC presentation. Nature *396*, 695–699.

Matsue, H., Edelbaum, D., Shalhevet, D., Mizumoto, N., Yang, C., Mummert, M.E., Oeda, J., Masayasu, H., and Takashima, A. (2003). Generation and function of reactive oxygen species in dendritic cells during antigen presentation. J. Immunol. *171*, 3010–3018.

Mellman, I., and Steinman, R.M. (2001). Dendritic cells: specialized and regulated antigen processing machines. Cell *106*, 255–258.

Nanda, A., Curnutte, J.T., and Grinstein, S. (1994). Activation of H+ conductance in neutrophils requires assembly of components of the respiratory burst oxidase but not its redox function. J. Clin. Invest. *93*, 1770–1775.

Pierre, P., Turley, S.J., Gatti, E., Hull, M., Meltzer, J., Mirza, A., Inaba, K., Steinman, R.M., and Mellman, I. (1997). Developmental regulation of MHC class II transport in mouse dendritic cells. Nature *388*, 787–792.

Raposo, G., Kleijmeer, M.J., Posthuma, G., Slot, J.W., and Geuze, H.J. (1997). Immunogold labeling of ultrathin cryosections: Application in Immunology, Chapter 208. In Handbook of Exp. Immunol. 5th ed. (Cambridge, MA: Elsevier), pp. 1–11.

Reeves, E.P., Lu, H., Jacobs, H.L., Messina, C.G., Bolsover, S., Gabella, G., Potma, E.O., Warley, A., Roes, J., and Segal, A.W. (2002). Killing activity of neutrophils is mediated through activation of proteases by K+ flux. Nature *416*, 291–297.

Segal, A.W. (2005). How neutrophils kill microbes. Annu. Rev. Immunol. *23*, 197–223.

Segal, A.W., and Coade, S.B. (1978). Kinetics of oxygen consumption by phagocytosing human neutrophils. Biochem. Biophys. Res. Commun. *84*, 611–617.

Segal, A.W., Geisow, M., Garcia, R., Harper, A., and Miller, R. (1981). The respiratory burst of phagocytic cells is associated with a rise in vacuolar pH. Nature *290*, 406–409.

Trombetta, E.S., Ebersold, M., Garrett, W., Pypaert, M., and Mellman, I. (2003). Activation of lysosomal function during dendritic cell maturation. Science *299*, 1400–1403.

Vowells, S.J., Sekhsaria, S., Malech, H.L., Shalit, M., and Fleisher, T.A. (1995). Flow cytometric analysis of the granulocyte respiratory

burst: a comparison study of fluorescent probes. J. Immunol. Methods *178*, 89–97.

Vulcano, M., Dusi, S., Lissandrini, D., Badolato, R., Mazzi, P., Riboldi, E., Borroni, E., Calleri, A., Donini, M., Plebani, A., et al. (2004). Toll receptor-mediated regulation of NADPH oxidase in human dendritic cells. J. Immunol. *173*, 5749–5756.

Winzler, C., Rovere, P., Rescigno, M., Granucci, F., Penna, G., Adorini, L., Zimmermann, V.S., Davoust, J., and Ricciardi-Castagnoli, P. (1997). Maturation stages of mouse dendritic cells in growth factor-dependent long-term cultures. J. Exp. Med. *185*, 317–328.

Yates, R.M., and Russell, D.G. (2005). Phagosome maturation proceeds independently of stimulation of toll-like receptors 2 and 4. Immunity *23*, 409–417.

Yilla, M., Tan, A., Ito, K., Miwa, K., and Ploegh, H.L. (1993). Involvement of the vacuolar H(+)-ATPases in the secretory pathway of HepG2 cells. J. Biol. Chem. *268*, 19092–19100.